The Journal of Experimental Biology 214, 2215-2225

doi:10.1242/jeb.050310

RESEARCH ARTICLE

Honeybee flight: a novel 'streamlining' response

Tien Luu[1,*], Allen Cheung[1], David Ball[1] and Mandyam V. Srinivasan[1,2]

[1]The University of Queensland, Queensland Brain Institute and School of Information Technology and Electrical Engineering, Brisbane, Queensland 4072, Australia and [2]ARC Centre of Excellence in Vision Science, The Australian National University, ACT 0200, Australia

*Author for correspondence (t.luu@edu.au)

Accepted 24 March 2011

SUMMARY

Animals that move rapidly through the air can save considerable energy by reducing the drag that they need to overcome during flight. We describe a novel 'streamlining' response in tethered, flying honeybees in which the abdomen is held in a raised position when the visual system is exposed to a pattern of image motion that is characteristic of forward flight. This visually evoked response, which can be elicited without exposing the insect to any airflow, presumably serves to reduce the aerodynamic drag that would otherwise be produced by the abdomen during real flight. The response is critically dependent on the presence of appropriate image motion everywhere within the large field of view of the insect. Thus, our results also underscore the importance of using panoramic stimulation for the study of visually guided flight in insects, and reveal the relative importance of various regions of the visual field in assessing the speed of flight through the environment.

Supplementary material available online at http://jeb.biologists.org/cgi/content/full/214/13/2215/DC1

Key words: insect flight, streamlining, vision, motion detection, virtual reality.

INTRODUCTION

It is abundantly clear that all creatures that move rapidly – in the air, on the ground or underwater – would save considerable locomotive energy if their bodies were shaped, or adjusted, to minimize the drag that is produced by the medium through which they move. For example, sharks, tuna and mackerel possess fusiform shapes that enable high swimming speeds to be achieved with relatively low drag (Schmidt-Nielsen, 1984; Bailey, 1997).

Although it is of interest to examine whether the bodies of certain animals have evolved to reduce drag, it is also pertinent to ask whether animals can actively change, or adapt, the shapes of their bodies to cope with the increased drag that inevitably accompanies higher speeds of locomotion. This would seem to be important because the force due to drag increases with speed, theoretically by as much as the square of the speed at which the body moves through the medium (Batchelor, 2000). In principle, an animal could achieve 'active' streamlining by sensing its motion through the medium either mechanically through, for example, mechanosensory hairs or organs to sense airspeed during flight (Goodman, 2003), or through vision, by sensing the motion of the image of the environment in the eye.

As an insect flies through the environment, its eyes experience various patterns of image motion – also known as optic flow patterns – which depend upon how the insect moves in relation to its surroundings. Research over the past 50 years has shown that insect flight is controlled by optic flow in a number of different ways. For example, the well-known optomotor response enables a flying insect to stabilize its attitude with respect to the world by sensing the patterns of optic flow that are generated by its rotations about the yaw, pitch and roll axes (or combinations thereof) and delivering appropriate commands to the flight motor system to counteract these rotations (Götz, 1965; Reichardt, 1969; Srinivasan and Bernard, 1977; Collett et al., 1993; Krapp and Hengstenberg, 1996; Egelhaaf et al., 2004). Fruit flies (David, 1979; David, 1982; Fry et al., 2009) and honeybees (Srinivasan et al., 1996; Baird et al., 2005) regulate their flight speed by holding constant the magnitude of the optic flow that is experienced by the eyes. Collisions with obstacles are avoided by detecting and steering away from regions in the visual field that are associated with unusually high image speeds (Srinivasan et al., 1993; Srinivasan and Zhang, 1997) or rapid expansion of the image (Tammero and Dickinson, 2002). Collision-free flight through narrow passages is achieved by balancing the magnitudes of the optic flow that are experienced by the two eyes (Srinivasan et al., 1991; Srinivasan et al., 1993; Srinivasan et al., 1996). Honeybees achieve smooth landings on horizontal surfaces by holding constant the rate of motion of the image of the surface during approach (Srinivasan et al., 2000).

Here we examine whether and how optic flow affects body posture during flight by filming tethered bees flying in a virtual reality arena that simulates the optic flow that would be generated by forward flight in a tunnel. We find that the simulated forward flight evokes a 'streamlining' response in which the bee raises its abdomen, lifting it progressively higher as the speed of the image is increased. This streamlining response is mediated visually, because it is displayed by tethered bees flying in still air and ceases when the image stops moving. Presumably, the streamlining response serves to reduce the aerodynamic drag that would otherwise be produced by the abdomen during real flight.

MATERIALS AND METHODS

Bees

Adult forager honeybees (*Apis mellifera*, Linnaeus 1758) were used in all of the experiments. All honeybees were collected from hives maintained by the Queensland Brain Institute at The University of

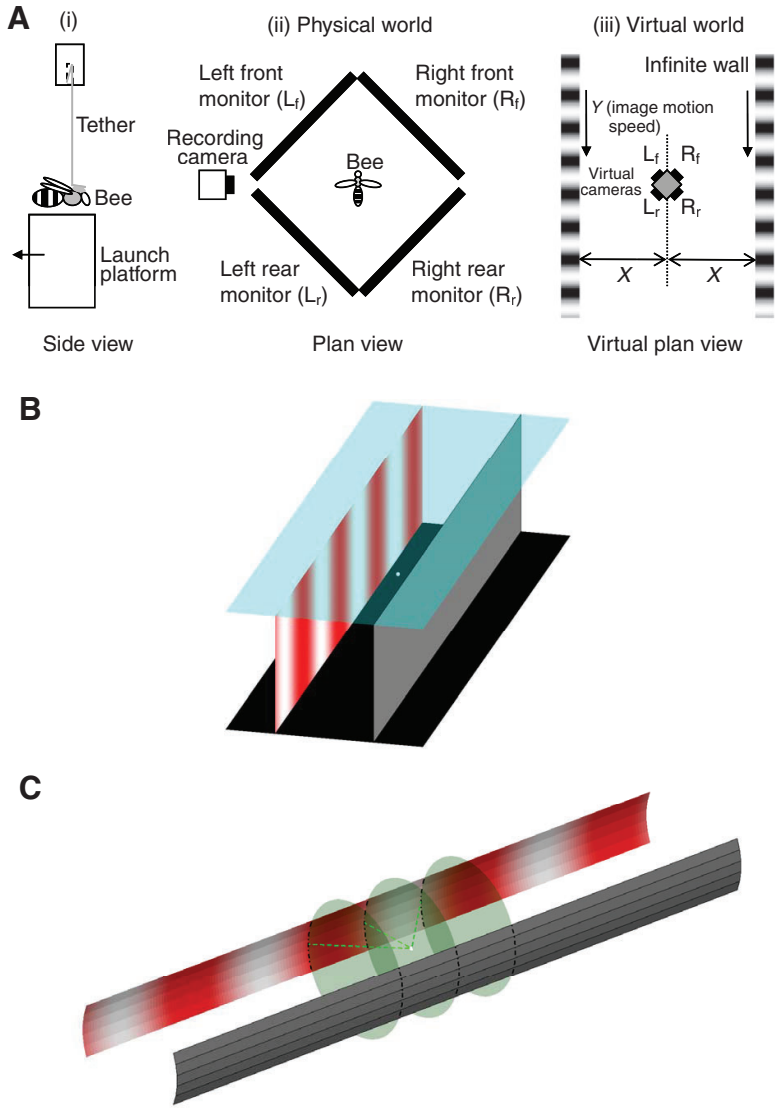

Fig. 1. The physical and virtual reality setup for investigating the streamlining response in tethered honeybees. (A) (i) Bees were tethered to the horizontal end of an L-shaped metallic rod. Flight was initiated by lowering a supporting platform. (ii) Each bee was placed in the centre of the arena composed of four monitors. A video camera was used to film a side view of the bee in flight. (iii) The virtual scene consisted of an infinite tunnel composed of two walls lined with vertically oriented red and white sinusoidal gratings. The bee was at a virtual distance of *X* units from each of the tunnel walls, and experienced virtual forward motion at a speed of *Y* units per display frame (see Materials and methods for further details). (B) Illustration of Virtual World 1, simulating flight in a tunnel of rectangular cross-section, with the ground rendered black and sky rendered blue. Because of the monitor dimensions, part of the elevational extent of the tunnel near 90 deg azimuth could not be displayed (not illustrated). (C) Illustration of Virtual World 2, simulating flight in a tunnel of circular cross-section, and showing the partitioning of the tunnel in the elevational and the azimuthal directions. The curvature of each tunnel wall was approximated by five flat axial strips of equal width. Note that owing to constraints imposed by the monitor dimensions, the virtual cylinder was truncated at the top and the bottom as illustrated in Fig. 6A, to allow the full elevational extent of the tunnel to be displayed at all azimuthal angles. The same black ground and blue sky planes were present in the Virtual World 2 but are not shown here, in order to allow an unobstructed view of the elevational and azimuthal partitions. Discs have been added in this schematic illustration to indicate the azimuthal tunnel partitions at 45, 90 and 135 deg along the horizontal plane (green dashed lines). Note that the virtual view point of the bee is denoted by a white dot in panels B and C.

Queensland, Australia. They were identified as those carrying pollen on their hind legs. The bees were anaesthetized in a refrigerator for 20–30 min, after which they were taken out one at a time for tethering.

Tethering

While the bee was anaesthetized, the base of an L-shaped metal rod (see Fig. 1Ai) was attached to the head (just above the ocelli) and thorax by a small globule of dental glue, which was cured using blue light (440–480 nm for ~40 s). Adhesion to the tether was facilitated by gently shaving the hair on the thorax using a scalpel blade. The bee was then housed in a Styrofoam box in which the temperature was maintained at 26–28°C. A beaker of water, placed inside the box, provided an environment with the appropriate humidity.

Experimental arena

Four 24 inch LCD monitors (Dell 2408WFP, Dell Australia, Sydney, Australia) were arranged on a table to form a square arena. A small (~2 cm) gap was provided at the two lateral corners of the arena to allow a video camera to film the bee in side view (Fig. 1Aii). The bee was tethered and positioned in the centre of the virtual environment by attaching the upper end of the L-shaped rod to an adjustable metallic arm (not shown). This arm allowed the head of the bee to be positioned in the centre of the arena, at a height midway between the base and top of the monitors. The bee faced one corner of the arena. The table was covered with a 60×90 cm sheet of black cardboard. All experiments were performed under fluorescent lighting.

Virtual reality environment

Images were created on the four monitors to provide a panoramic virtual environment (Fig. 1Aiii). The LCD monitors were driven by a PC (Intel Quad Core CPU Q9300 2.5 GHz, 3 GB RAM, Windows XP 2002, Dell Australia) with two dual head NVIDIA GeForce 8800 GT video cards (Dell Australia). The monitors had the following settings: 1920×1200 pixel resolution, 60 Hz refresh rate. Because the monitors used LCD displays, there was no 60 Hz flicker. This was confirmed by direct measurement of the display intensity using a photodiode sensor with a frequency response extending to the MHz range.

A program was written that simulated the visual effects of the movement of an observer within a custom-designed virtual world.

The virtual world consisted of an (apparently) infinite tunnel with a blue ceiling, a dark floor and side walls lined with a sinusoidal grating composed of alternating red and white bars. The red bars would have appeared as (almost) black bars to the bee, because the colour red falls outside the bee's visible spectrum (Menzel and Blakers, 1976; Chittka et al., 1993). Red was used rather than black to facilitate viewing and filming of the tethered bee against the background of the visual display. Experiments were conducted using two types of virtual worlds.

Virtual World 1

In this world, illustrated in Fig. 1B, the walls of the tunnel were vertical planes 1 unit high, positioned 0.4 units on either side of the viewpoint (virtual camera position), creating a theoretical maximum vertical extent of 1.75 rad (100 deg) from the viewpoint of the tethered bee. Because this was a virtual tunnel, the linear units were of arbitrary units. For example, a real tunnel 20 cm wide would have corresponding walls 25 cm high.

Virtual World 2

To further investigate the contribution of optic flow from different regions of an infinite tunnel to the streamlining response, we constructed a variant of the virtual tunnel described above. In a tunnel with a rectangular cross-section (as described above), the magnitude of the optic flow that is experienced by the bee would decrease as the elevation of the direction of view is increased (specifically, as the cosine of the elevation angle). To eliminate this effect, we used a virtual tunnel with a circular cross-section (Virtual World 2), so that the bee experienced visual flow that would be equivalent to flight through the central axis of an infinitely long cylinder (Fig. 1C). With this configuration, the magnitude of the optic flow was independent of elevation for all points on the tunnel surface that are at a given virtual axial distance from the bee, as illustrated in Fig. 1C and Fig. 6A. The virtual tunnel could also be subdivided into sections along the axis of the cylinder, thus permitting investigation of the variation of sensitivity in the azimuthal plane as illustrated in Fig. 1C and Fig. 7A.

Note that by elevation we mean the angle of elevation in relation to the cylindrical geometry as illustrated by Fig. 1C. By azimuth we mean the semi-apical angle of the cone that intersects the virtual cylinder to define the length of the cylindrical subsections into which the tunnel was divided, as illustrated by Fig. 1C.

A further modification from the rectangular virtual tunnel used in Virtual World 1 was to reduce the vertical extent of the tunnel walls so that the entire wall could be displayed at all azimuth angles. Because of the physical sizes of the monitors and the cylindrical geometry of the tunnel, this resulted in a maximum elevational extent of approximately ±0.40 rad (i.e. 23 deg above and below the horizontal plane). Other stimulus parameters (grating spatial period and range of stimulus speeds) were identical to those for Virtual World 1. The curvature of each wall was approximated by five axial strips of equal width, as illustrated in Fig. 1C and Fig. 6A. Within the space of each axial strip, smaller rectangles (subpanels) were used as needed to display a texture covering a fractional extent in elevation or azimuth. The details of the various stimuli used are described in Fig. 6A and Fig. 7A.

During the experiments, some subpanels displayed a moving grating, which generated optic flow. The remaining subpanels had zero contrast and the same mean luminance as the moving gratings, and generated no optic flow. Preliminary experiments (not shown) revealed that the magnitude of streamlining response that was evoked by a given stimulus condition did not depend upon whether the non-stimulating regions carried a stationary grating, displayed zero contrast or were dark (black). Therefore, in all of the experiments carried out using Virtual World 2, the non-stimulating regions had zero contrast and the same mean luminance as the moving gratings.

Note that the monitor's plastic frame interrupted the display of the virtual tunnels in four locations: anterior, posterior, perpendicular to the right and perpendicular to the left of the tethered bee. Each pair of adjacent monitor frames subtended ±2.1 deg in azimuth along the horizon plane. These interruptions were accounted for setting the virtual camera horizontal viewing angle to 85.8 deg. By using a diamond configuration for the four monitors (see Fig. 1A), for a 0.8 unit wide tunnel, the visible portion spanned ±10.8 units along the axis of the infinite tunnel, with approximately 0.03 units not displayed to the right and left of the bee.

Display generation

The program to create the displays was written in C++ and used DirectX API software (Microsoft, USA) to create four 'viewports' of the virtual world, each displayed by one monitor, with the virtual camera position geometrically matched to the centre of the arena. Each monitor displayed one quadrant of the virtual world: forward right, forward left, rear left and rear right. A software interface, written in Python, enabled customization of the virtual world and control of the virtual position and motion of the observer within it. For a bee flying along a virtual tunnel, the maximum image velocity as experienced by the eyes [maximum optic flow rate (OFR)] occurs in the lateral viewing direction, i.e. in a viewing direction at 90 deg to the direction of flight. For a simulated linear grating speed of Y units frame^{-1}, a frame rate of 60 Hz and a simulated flight along a trajectory that is X units from either wall, this maximum OFR (deg s^{-1}) is given by:

$$\mathrm{OFR}\ (\mathrm{deg}/s) = \left(\frac{60Y}{X}\right)\left(\frac{180}{\pi}\right). \quad (1)$$

We used a stimulus protocol that simulated flight at a progressively increasing speed, namely, Y=0.02, 0.03, 0.04, 0.05, 0.06, 0.07, 0.08, 0.09 and 0.1 units frame^{-1}. This staircase of simulated flight speeds generated the following OFRs: 172, 258, 344, 430, 516, 602, 688, 773 and 859 deg s^{-1}, respectively. Each epoch of stimulus speed was 8 s in duration, thus producing a stimulus that lasted for 72 s in each trial.

To estimate the frequency of display artifacts such as frame dropouts, we used a grating with a sawtooth intensity profile to texture the polygons using the tunnel configuration requiring the most polygons (corresponding to Virtual World 2, azimuth stimulus AZ3, illustrated in Fig. 7). During a simulated flight at constant speed, assuming a smooth render rate, we expected an intensity profile that corresponds to the grating profile. When using a Silicon PIN Photodiode (OSRAM Opto Semiconductors, Pennant Hills, Australia), the linear intensity profile of the sawtooth prevented possible confusion between slowly changing pixel intensities (e.g. near turning points of sinusoidal intensity functions) and a failure to render the next frame. Furthermore, during each frame, we observed faster kinetics of equilibration when pixel intensity was increasing between frames than when decreasing, likely reflecting the physical properties of the LCD. We therefore only analyzed the rising phase of the sawtooth intensity profile. To maximize the proportion of this rising phase, the sawtooth profile was asymmetric. Hence each cycle consisted of an ascending phase where intensity increased linearly from zero to maximum, followed by a step drop

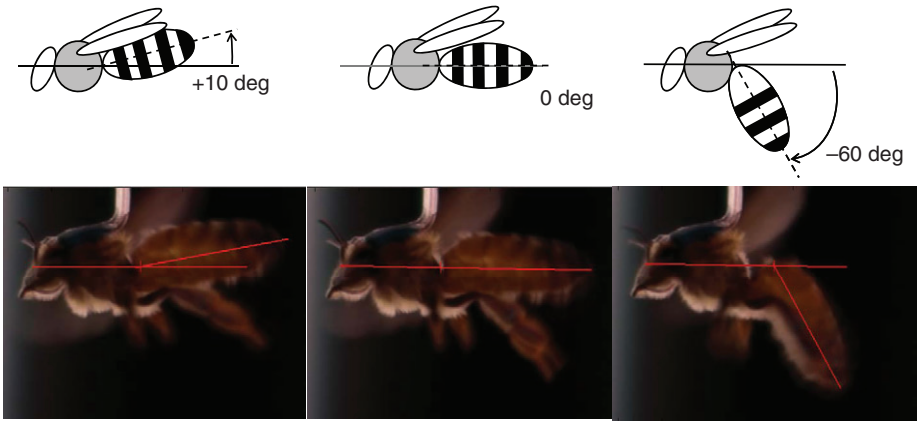

Fig. 2. Illustration of the measurement of the streamlining response, defined as the orientation of the abdomen relative to the thorax. The sketches illustrate the definition of the response, and the images give three examples of how this is used to measure the response. See 'Data acquisition and image analysis' for details.

to zero intensity, followed by a short pause. Only intensity changes occurring completely within each ascending phase were assessed, typically approximately eight per cycle. In an approximately 75 s continuous period, there were 4008 frames assessed using this protocol, with a total of 15 randomly scattered anomalies detected.

The anomalies were either pauses at one particular intensity for twice the duration of a standard frame epoch (possible skipped frame) or an incomplete change in intensity. It is likely that at least some of these anomalies were artifacts due to the unavoidable spatial averaging of intensity by the photodiode sensor. Therefore, this error rate of 0.37% is likely to be a 'worst case' estimate, making it highly improbable that it influenced the temporally averaged responses reported here in any substantial way.

Calibration of stimulus contrast

Sinusoidal gratings of 10 different contrast levels were used. These contrasts (as defined below) were nominally set to 1.0, 0.75, 0.5, 0.4, 0.3, 0.25, 0.2, 0.15, 0.1 and 0.0, for both the green and blue channels in the 24 bit RGB bitmaps generated using MATLAB (MathWorks, Natick, MA, USA). The red channel was kept constant at its maximum value over the entire bitmap. These grating bitmaps were tessellated to build the long virtual tunnels (described above). However, subsequent measurement and calibration of the various gratings, as described below, revealed that the actual contrasts of these gratings were 0.72, 0.54, 0.36, 0.29, 0.22, 0.18, 0.14, 0.11, 0.07 and 0. The actual values are used when reporting the results.

The contrasts of the gratings were measured as follows. First, the radiant spectrum of the monitors was measured using an Ocean Optics USB2000+ spectrometer (Lastek, Adelaide, Australia) calibrated for wavelength and intensity. Spectra were measured for illumination from a small patch within the centre of the white bar of the sinusoidal grating, as well as within the centre of the red bar. The relative photon flux emitted by each of these patches was obtained by integrating their respective spectra over a spectral window of 300–600 nm, which represents the visible spectrum of the honeybee (Menzel and Blakers, 1976; Chittka et al., 1993). Denoting the results of this integration for the white and the red bars by I_{max} and I_{min}, respectively, the contrast (C) of the grating was calculated as $C=(I_{max}-I_{min})/(I_{max}+I_{min})$. This quantity, known as the Michelson contrast, is the commonly used measure of contrast for sinusoidal gratings (Michelson, 1927). It can assume a maximum value of 1.0 when the dark bar emits no light ($I_{min}=0$) and a minimum value of 0 when the dark and bright bars have the same intensity ($I_{max}=I_{min}$).

In all experiments but one (Fig. 5A,B), the Michelson contrast of the grating was set at a high value ($C=0.72$). In one experiment, which investigated the effect of stimulus contrast, response *versus* speed curves were obtained for a series of contrasts, as shown in Fig. 5.

Data acquisition and image analysis

A Samsung video camera (VP-HMX20C, 25 frames s^{-1}, 1920×1080 pixel resolution; Samsung Australia, Brisbane, Australia) was used to film the side view of the bee. The video clips were analyzed to measure the orientation of various parts of the body, using a MATLAB digitization program written in-house. The program computed the orientation of the line joining any two manually digitized points in the image. It was used to measure the orientation of two lines. One line, connecting the head to the thorax, was defined as the orientation of the thorax. Another line, connecting the front and rear ends of the abdomen, was defined as the orientation of its long axis. The program calculated the difference between these two orientations (Fig. 2). This difference, representing the orientation of the abdomen relative to the thorax, was defined as the abdomen angle, or the response. The response was positive or negative, according to whether the abdomen was elevated or depressed relative to the thorax. The image analysis involved overlaying (superimposing) all 25 frames of each second to measure the average abdominal position over this time period. Initial tests revealed that this procedure yielded similar results to those obtained by averaging 25 individual measurements of abdominal position over each second. The measurement of abdominal angle was repeated for each of the 72 s of the flight protocol. The abdominal angles reported throughout this study were of the honeybee's steady-state response to each of the nine stimulus speeds. The response was calculated as the mean abdominal angle measured during the last 4 s of each 8 s epoch of stimulus speed. Typically, the abdominal response reached a new steady state within 1–3 s following each new stimulus speed (data not shown).

Statistical analysis

All statistical analyses were performed using the software package SPSS/PASW Statistics 18.0 (SPSS Inc., IBM Australia, West Pennant Hills, Australia). In each case, we first performed two-way repeated measures ANOVA to investigate the effect of each independent variable, at all OFRs of the stimulus protocol. If a significant effect was detected, *post hoc* pairwise comparisons (*t*-tests, with Bonferroni adjustment for the family-wise Type I error rate) were performed. Note that for the main effect of interest in each case, there was no detectable violation of the sphericity assumption (using Mauchly's test of sphericity), hence the degrees of freedom were not adjusted. All statistical results for the main effect of interest are shown in the supplementary material.

Comparison of responses elicited by two and four monitors

Abdominal responses were compared across the various two-monitor configurations and across two- and four-monitor configurations, all at full grating contrast (C=0.72). Only responses from honeybees that experienced all the different configurations were used for this particular comparison (N=7). Because a significant effect was only detected when the four-monitor data were included, *post hoc* tests were only performed in the latter case. These statistical results are shown in supplementary material Tables S1 and S2.

Variation of response with stimulus contrast

Abdominal angles were compared across the various stimulus contrast levels (0.0, 0.07, 0.11, 0.14, 0.18, 0.22, 0.29, 0.36, 0.54 and 0.72), all using the four-monitor configuration. Only responses from honeybees that experienced all the different contrasts (including 0) were used for this particular comparison (N=6). These statistical results are shown in supplementary material Tables S3–S5.

Flight initiation

For each flight trial, a tethered honeybee was placed in the centre of the arena and a platform (Fig. 1) was raised from under the bee until all of the bee's tarsae made contact with it, with the legs in their natural resting position. As soon as the visual stimulus was started, the platform was retracted from under the bee. At the end of the visual stimulus, the platform was restored to its pre-flight position so that the bee's legs were again resting on it, thus preventing further flight. The platform was covered with wax paper (which was frequently replaced) to ensure a firm but smooth support that could not be gripped by the bee's tarsal hooks, thus ensuring trouble-free release of the feet at the onset of flight. After each flight the bee was fed 10 µl of 1 mol l^{-1} sucrose solution and returned to the humid box.

RESULTS

We found that in all bees tested, the action of removing the platform from under the bee's legs immediately triggered wing beat activity. This is the well-known tarsal reflex (Fraenkel, 1932; Chadwick, 1953). At this instant, the abdomen would also drop and assume a hanging orientation. Bees would then occasionally fly for a few seconds. However, combining the platform removal with the onset of a moving visual stimulus enhanced the duration of flight considerably, typically by at least 2 min, as we shall describe below. Hence, our protocol was to place the tethered honeybee in the centre of the arena, rest it comfortably on the platform and then commence the stimulus motion as soon as possible after platform withdrawal (typically within 1 s). The experiments described below (in the first four sections) used Virtual World 1.

Honeybees only exhibit flight behaviour during simulated forward motion

Withdrawal of the platform always triggered wing beat activity. However, this activity typically ceased seconds thereafter if there was no image motion. The abdomen would then hang almost vertically and often curl inwards toward the head (Fig. 3). Similar responses were observed when honeybees were exposed to backward image motion, namely, image motion that simulated backward flight. In contrast, even on the very first test flight, the majority of honeybees (76 out of 101) that experienced forward image motion – image motion that simulated forward flight – exhibited continuous flight for the entire duration of the visual stimulus. Presentation of forward image motion in the two front monitors and backward image motion in the two rear monitors – or *vice versa* – also evoked no flight (data not shown).

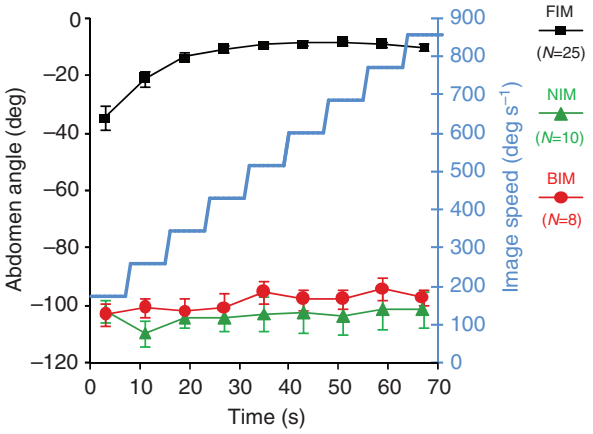

Fig. 3. Comparison of streamlining responses induced by forward image motion (FIM), no image motion (NIM) and backward image motion (BIM). The stimulus was Virtual World 1. The blue staircase displays the progressively ascending stimulus speed (see Materials and methods). Data are mean abdomen angles ± s.e.m. Note the comparatively small variability in the responses when bees were experiencing forward image motion.

A novel streamlining response observed during simulated forward image motion

Bees presented with forward image motion responded not only with wing beat activity, but also with a streamlining response. As the speed of the image motion was increased, the position of the abdomen would rise progressively and then remain in the elevated position for the rest of the trial (Fig. 3; supplementary material Movie 1). The abdomen reached its highest elevation (approximately –10 deg) at an image speed of 430 deg s^{-1} and remained at this elevation for all higher speeds, up to the maximum speed of 859 deg s^{-1}. Thus, at speeds beyond 430 deg s^{-1}, the streamlining response was maximal and approximately independent of stimulus speed.

Panoramic motion vision in honeybees

Bees were also tested in the same arena with different combinations of only two active monitors (the other two monitors were switched off, creating a black display). All tests were conducted using the same stimulus protocol of ascending image speed. The bees exhibited a streamlining response even with the two monitor setups. However, in this case they flew less consistently and for shorter periods. Only 13 out of 57 bees tested (23%) flew on the very first flight when stimuli were presented only in the two front monitors, with the two rear monitors turned off. In another set of tests, only 22 out of 106 bees tested (21%) flew on the first flight when the two rear monitors were removed, exposing the stationary environment of the laboratory in the rear visual field.

Fig. 4 shows the relationship between the response and stimulus speed for various combinations of stimulation with two monitors: (1) left and right front fields, (2) left and right rear fields, (3) left front and right rear fields, and (4) right front and left rear fields. Statistical analyses were performed to examine whether the abdominal responses for all of these four different two-monitor configurations differed significantly. The two-way repeated measures ANOVA did not reveal any significant main effect of

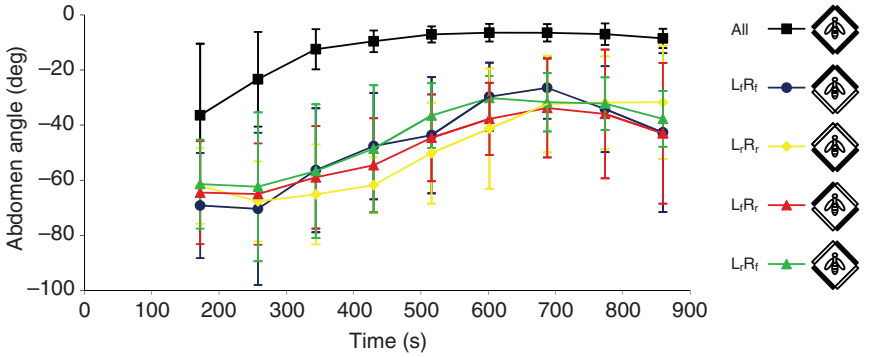

Fig. 4. Streamlining responses of tethered bees in experiments using various configurations of two monitors (colored symbols) compared with the four-monitor configuration (black squares). The stimulus was Virtual World 1. All flights were presented with the ascending image motion speed protocol. Data are mean abdomen angles ± s.d. Data are only from bees that experienced all five monitor configurations (N=7).

monitor configuration ($F_{3,18}$=0.44, P=0.73; supplementary material Table S1).

However, it is clear that, in comparison with the results obtained using four monitors, the abdominal responses obtained with two monitors are consistently lower. This is also reflected in the statistical results. We find that there is a significant main effect of monitor configuration ($F_{4,24}$=19.62, P<0.001; supplementary material Table S2) when the data set includes responses from four- and all two-monitor configurations. *Post hoc* pairwise comparison of the monitor configurations at each OFR showed significant differences between the four-monitor configuration and each two-monitor configuration (P<0.01 with Bonferroni correction in all cases; supplementary material Table S2).

Furthermore, whereas the curve for four monitors is essentially flat for speeds greater than 430 deg s^{-1}, the two-monitor curves exhibit a peak at stimulus speeds between 602 and 773 deg s^{-1} (Fig. 4). With two monitors, similar response–speed curves are obtained regardless of the configuration of the monitors – all four configurations yielded similar results (Fig. 4).

One should consider the possibility that the intermediate peak observed in the two-monitor tuning curves arises as a result of fatigue during flight through the prolonged (72 s) stimulus protocol, causing the response to diminish at higher speeds. However, this is unlikely because the mean of all of the two-monitor responses at the time of 52 s (when the stimulus speed is 688 deg s^{-1}) is not statistically different from the mean at 66 s (when the stimulus speed is at its highest value of 859 deg s^{-1}) (t-test, P>0.05; Fig. 4). Furthermore, preliminary tests using a constant stimulus speed over the entire 72 s period showed no signs of response fatigue (data not shown). Indeed, bees were frequently observed to fly streamlined for periods of over 2–3 min.

Effect of stimulus contrast on the streamlining response

How sensitive is the streamlining response to variations in the contrast of the visual environment? This was investigated by conducting experiments with the four-monitor configuration using the standard stimulus protocol (as in the experiments shown in Figs 3 and 4) for different Michelson contrasts of the grating. The results

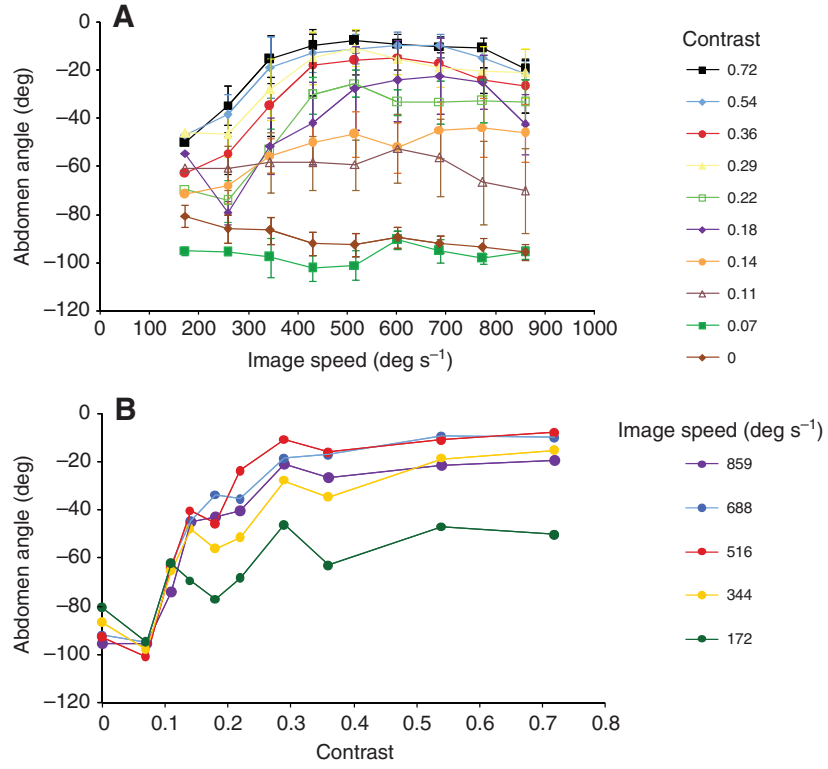

Fig. 5. Effect of stimulus contrast on the streamlining response using the four-monitor configuration. (A) Variation of abdomen orientation with stimulus speed for 10 different contrasts. Data are mean abdomen angles ± s.e.m. (N=6). (B) Re-plot of a subset of the data of Fig. 5A, showing the variation of the mean abdomen angle with stimulus contrast. For clarity, the data are shown only for every second image speed, and error bars are omitted because they are shown in A. The stimulus was Virtual World 1.

are shown in Fig. 5. The profiles of the curves for the four highest contrasts, namely C=0.72, 0.54, 0.36 and 0.29, are very similar in shape and height (Fig. 5A). Statistical analyses were performed to examine whether the abdominal responses for all of these four grating contrasts differed significantly. These analyses did not detect any significant main effect of contrast ($F_{3,15}$=1.47, P=0.26). Consistent with the ANOVA results, the corrected *post hoc* pairwise comparisons between the four highest contrast conditions did not show any significant differences (in all cases, P>0.45; supplementary material Table S3). When the abdominal responses obtained from the same bees for a grating contrast of 0 were included for comparison, results showed that there was a significant main effect of contrast ($F_{4,20}$=53.24, P<0.001). *Post hoc* pairwise comparisons of contrast conditions at each OFR showed significant differences between each zero contrast and all of the four highest contrast conditions (in all cases, P<0.005 with Bonferroni correction; supplementary material Table S4).

However, the profiles for the lower contrasts, namely C=0.22, 0.18, 0.14, 0.11 and 0.07, are each significantly lower than each of the curves for the higher contrasts (P<0.05; supplementary material Table S5), except for the leftmost point that corresponds to the lowest stimulus velocity and represents the start of the flight (Fig. 5A). Although there is no statistically significant difference between the responses obtained for the contrasts C=0 and 0.07 ($F_{1,5}$=1.52, P=0.272), there is a significant difference between each of these responses and those at C=0.11 (*vs* C=0, $F_{1,5}$=8.45, P=0.033; *vs* C=0.07, $F_{1,5}$=8.20, P=0.035). Thus, under our stimulus conditions, the threshold contrast for the streamlining response is between 0.07 and 0.11.

Fig. 5B is a re-plot of a subset of the data of Fig. 5A, showing the variation of the mean abdomen angle with stimulus contrast. These curves confirm that the threshold for the streamlining response lies between 0.07 and 0.11, and that, for each image speed, the response reaches and maintains its maximum value at all contrasts above 0.3. Thus, the streamlining response is relatively robust to changes of stimulus contrast, in the mid-to-high contrast range of 0.3–0.72. The threshold contrast for the streamlining response appears to be in the vicinity of 0.1.

Effect of location and extent of visual stimulation on the streamlining response

We have shown above that panoramic stimulation of the visual field is much more effective than stimulation of one half of the visual field in eliciting the streamlining response. To investigate the sensitivity of the streamlining repose to stimulation in different regions of the visual field, we investigated the effectiveness of different sections of the virtual tunnel in eliciting a streamlining response. This was done using a virtual world composed of a tunnel with a circular cross-section (Virtual World 2).

The investigation was carried out using two different sets of experiments. In the first set, we investigated the variation of sensitivity in the vertical (elevational) plane by subdividing the surface of the virtual tunnel into a number of axial strips and presenting optic flow in selected combinations of these strips, as illustrated in Fig. 1C and Fig. 6A. All of the combinations were left–right symmetric. The total elevational extent of the virtual tunnel was 46 deg (±23 deg above and below the horizontal plane).

With full stimulation [optic flow present in all five axial strips (S1–S5); stimulus EL1, Fig. 6A], the streamlining response displayed maximal strength at almost all image velocities (black squares, Fig. 6B), as in the experiments using Virtual World 1 (e.g. Figs 4, 5). The mean response was consistently lower at all image velocities

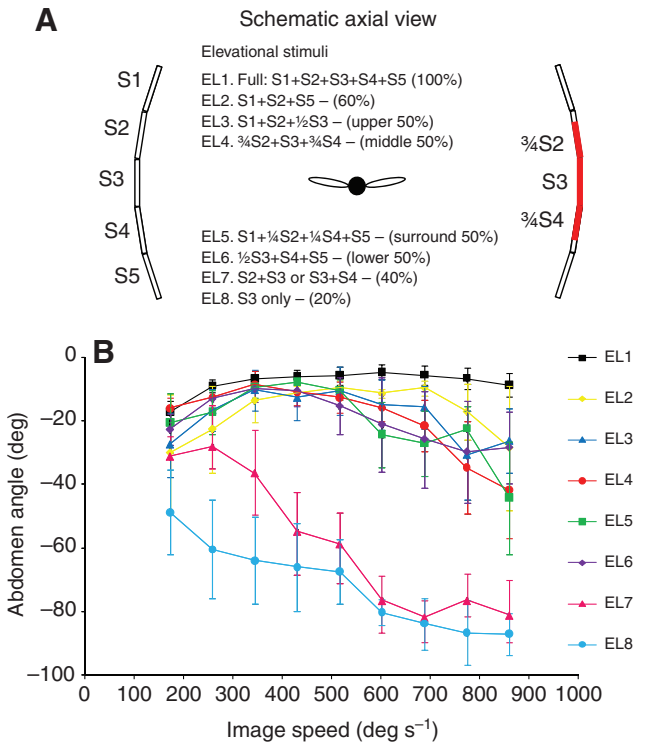

Fig. 6. Effect of elevational position and extent of stimulus on the streamlining response. The stimulus was Virtual World 2. (A) Illustration of the subdivision of the virtual tunnel into five axial strips (S1, S2, S3, S4 and S5), and the use of grating motion in various combinations of these strips to achieve stimulation at various elevational angles and various elevational extents. The red sections illustrate stimulus EL4 (as an example), which presents optic flow in the middle 50% of the tunnel surface. (B) Variation of streamlining response with stimulus speed for each of the stimulus conditions. Data are mean abdomen angles ± s.e.m. (N=6).

greater than 172 deg s^{-1} when flow was present only in the upper half of the tunnel (stimulus EL3, Fig. 6A; blue triangles, Fig. 6B), only the lower half (stimulus EL6, Fig. 6A; purple diamonds, Fig. 6B), only the middle half (stimulus EL4, Fig. 6A; red circles, Fig. 6B) or only the surrounding half (stimulus EL5, Fig. 6A; green squares, Fig. 6B). However, these differences were not statistically significant ($F_{4,16}$=0.97, P=0.45). In particular, none of the responses to the four 50% elevational stimuli were significantly different from each other ($F_{3,12}$=0.38, P=0.77). It appears, therefore, that the sensitivity of the streamlining response is uniformly distributed in the elevational plane – the responses elicited by simulation in the upper, lower and middle halves of the tunnel are all virtually identical. However, these responses are not significantly different from those elicited by full stimulation (stimulus EL1). Therefore, these findings suggest that the variation of the response in the elevational direction is a saturating function of the area of stimulation within the tunnel surface, but does not depend upon the location of this area. This is consistent with the experimental observation that increasing the area of stimulation from 50 to 60% (stimulus EL2, Fig. 6A) elicits a slightly stronger response in the high-velocity regions of 600–800 deg s^{-1} (yellow diamonds, Fig. 6B). However, lowering the area of stimulation below 50% causes a precipitous drop in the response; 40% stimulation (stimulus EL7, Fig. 6A, involving only two strips) produces a significantly weaker response (pink triangles, Fig. 6B) at all stimulus velocities except the two

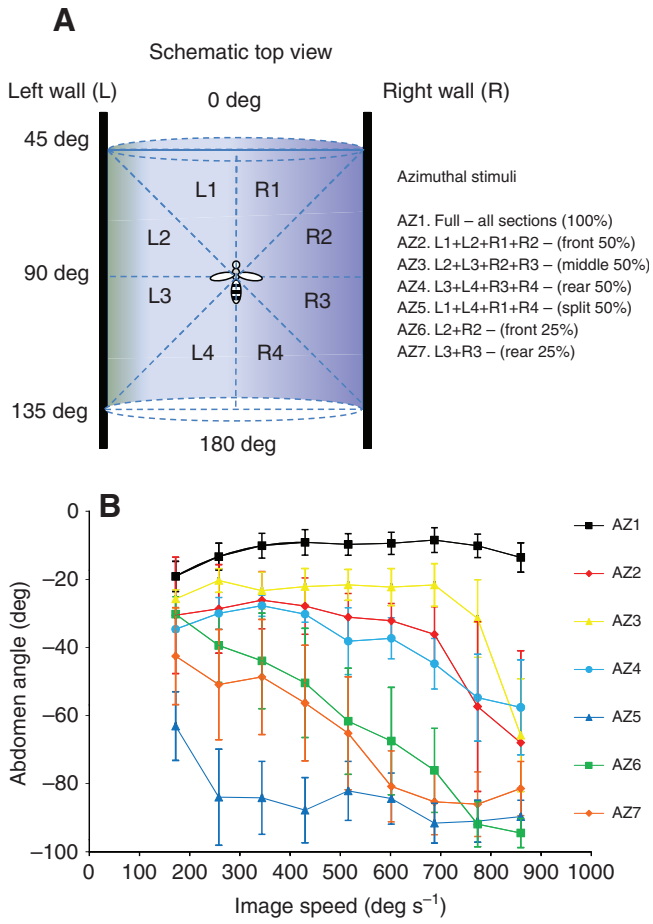

Fig. 7. Effect of azimuthal position and extent of stimulus on the streamlining response. The stimulus was Virtual World 2. (A) Illustration of the subdivision of the virtual tunnel into four sections along the axis of the cylinder, denoted by L1, L2, L3 and L4 on the left-hand side and R1, R2, R3 and R4 on the right-hand side. Each of these sections subtends 45 deg in azimuth at the eyes of the bee. Grating motion is presented in various combinations of these sections to achieve stimulation at various azimuthal angles and extents. (B) Variation of streamlining response with stimulus speed for each of the stimulus conditions. Data are mean abdomen angles ± s.e.m. (N=5).

lowest ones in the range 100–300 deg s^{-1} ($F_{4,16}$=30.49, P<0.001; see supplementary material Table S6 for pairwise comparisons). In this case, data from the upper 40% (S2+S3) and the lower 40% (S3+S4) of the field were statistically indistinguishable (t-test, P>0.68) and were therefore pooled to obtain the results shown for stimulus EL7. Reducing the area of stimulation to just one strip (S3 only, stimulus EL8, Fig. 6A) produces the weakest response. This is true for single-strip stimulation at each elevation (data not shown).

In summary, this set of experiments indicates that, for a stimulus consisting of a virtual tunnel, the sensitivity of the streamlining response to optic flow has the following properties. In the elevational direction, the streamlining response depends, to a first approximation, upon the area of the region of stimulation that is provided by the tunnel surface, but not upon where in the elevational plane this region is located (at least within the ±23 deg range of elevations that was investigated in these experiments). Furthermore, the responses that are induced by various sub-regions of the stimulus appear to be spatially summed in a nonlinear fashion, with the response tending to stay high as long as the area of stimulation is at or above 50%, but decreasing dramatically when this area is reduced to values lower than 50%.

In the second set of experiments, we investigated the variation of sensitivity in the horizontal (azimuthal) plane by subdividing the virtual tunnel into a number of cylindrical sections, and presenting optic flow in selected combinations of these sections as illustrated in Fig. 1C and Fig. 7A. All of the combinations were front–rear symmetric. The virtual tunnel was infinitely long, providing a total azimuthal extent of 180 deg on either side. The statistical results from this set of experiments are summarized in supplementary material Table S7.

With full stimulation (optic flow present in all of the sections, L1–L4 and R1–R4; stimulus AZ1, Fig. 7A), the streamlining response displayed maximal strength at almost all image velocities (black squares, Fig. 7B). This response is identical to that elicited by the full stimulus shown in Fig. 6A (black squares, Fig. 6B), because the two full stimuli are identical.

When the stimulus was restricted to a cylindrical section covering the lateral fields L2, L3, R2 and R3, spanning a total azimuthal angle of 90 deg on either side (stimulus AZ3, Fig. 7A), the response was slightly but significantly lower than that corresponding to the full-field stimulation ($F_{1,4}$=7.80, P=0.049; yellow triangles, Fig. 7B). When the stimulus was restricted to a cylindrical section covering the frontal fields L1, L2, R1 and R2, spanning a total azimuthal angle of 90 deg on either side (stimulus AZ2, Fig. 7A), the response was significantly lower still ($F_{1,4}$=12.54, P=0.024; red diamonds, Fig. 7B). This response was comparable to that obtained when the stimulus was restricted to a cylindrical section covering the rear fields L3, L4, R3 and R4, spanning a total azimuthal angle of 90 deg on either side (stimulus AZ4, Fig. 7A; blue circles, Fig. 7B). There was no significant difference between the responses elicited by stimuli AZ2 and AZ4 at all stimulus velocities ($F_{1,4}$=0.004, P=0.955). Thus, there appears to be symmetry about the coronal plane (center disc in Fig. 1C) in the sensitivity of the streamlining response to optic flow. When the stimulus region was further restricted to the frontolateral regions L2 and R2, covering an azimuthal extent of 45 deg on either side (stimulus AZ6, Fig. 7A), the response was significantly lower again ($F_{1,4}$=22.17, P=0.009; green squares, Fig. 7B). This response was comparable to that obtained when the stimulus region was restricted to the rear lateral regions L3 and R3, again covering an azimuthal extent of 45 deg on either side (stimulus AZ7, Fig. 7A; orange diamonds, Fig. 7B). There was no significant difference between the responses elicited by stimuli AZ6 and AZ7 at all stimulus velocities ($F_{1,4}$=3.85, P=0.121). This result is again indicative of a rostrocaudal symmetry in the sensitivity of the response. Finally, when the stimulus was restricted to just the extreme frontal regions (L1 and R1) and the extreme rear regions (L4 and R4), covering an azimuthal extent of 90 deg on either side (stimulus AZ5, Fig. 7A), the response was the weakest of all (blue triangles, Fig. 7B). In this case, the response was practically non-existent, and was substantially and significantly weaker than those elicited by stimuli AZ6 and AZ7 at all stimulus velocities below 500 deg s^{-1} ($F_{2,8}$=6.13, P=0.024). This is despite the fact that this stimulus covered the same azimuthal extent (90 deg on either side) as stimulus AZ3, which evoked a response that was much larger.

In summary, the results of this set of experiments indicate that, for a stimulus consisting of a virtual tunnel, the sensitivity of the streamlining response to optic flow is greatest in the lateral fields of view and lowest in the frontal and rear fields of view. Furthermore, the variation in sensitivity is symmetrically distributed about the coronal plane.

DISCUSSION

The streamlining response

Our results have revealed, for the first time, the existence of a visually driven streamlining response in flying insects. This response, which can be elicited without exposing the insect to any airflow, presumably serves to reduce the aerodynamic drag that would otherwise be produced by the abdomen during real flight. Although earlier studies with flying insects have documented elevation of the abdomen during flight [e.g. in moths (Willmott and Ellington, 1997), bumblebees (Dudley and Ellington, 1990), *Drosophila hydei* (David, 1978) and honeybees (Nachtigall et al., 1971)], they observed this elevation in free, un-tethered flight. Hence, it is difficult to ascertain from these studies whether the raising of the abdomen was meditated by visual input, mechanosensory signals driven by the wind, or simply passive mechanical raising of the abdomen by the wind. However, Zanker reports a cursory observation of a small difference (±2 deg) in abdominal deflection between backward image motion and forward image motion in *Drosophila melanogaster* (Zanker, 1988). Our study demonstrates comprehensively that the streamlining response can be elicited by a visual stimulus alone – namely, a moving pattern – and documents its properties.

The importance of panoramic and contextually consistent image motion

The streamlining response is highly selective to the direction of motion of the visual pattern. Forward image motion (motion in the direction that would be experienced during forward flight) creates a pronounced elevation of the abdomen. However, a stationary pattern, or a pattern that moves in the opposite direction (simulating backward flight) does not elicit any response – the abdomen remains in its lowered state (Fig. 3).

Panoramic stimulation with image motion seems to be crucial for eliciting a strong streamlining response. With four monitors, the response is significantly and substantially stronger than that measured with two monitors, at all stimulus speeds (Fig. 4). The four-monitor stimulus produces a streamlining response that increases steadily with stimulus speed up to a speed of approximately 400 deg s^{-1}, and then remains constant at this maximum value for all higher stimulus speeds. The two-monitor stimulus, however, yields a bell-shaped curve for response *versus* stimulus speed, exhibiting a peak at stimulus speeds in the range of 602–773 deg s^{-1}, regardless of the particular configuration of the two stimulating monitors (Fig. 4).

These findings reveal that, when studying visually evoked responses in flying insects, it is important to ensure that the stimulation covers all or as much of the visual field of the insect as possible. Panoramic visual stimulation, which is what an insect would experience during actual flight in a real environment, reveals response properties that are very different from those produced by visual stimulation of restricted regions of the visual field. Consequently, many of the earlier studies of visually evoked behaviour in insects that did not use panoramic, or nearly full-field, stimulation would have to be reassessed.

Spatial summation of movement signals in the generation of the streamlining response

What causes four-monitor stimulation to be more effective than two-monitor stimulation? A simple possibility is that the responses of movement-detecting neurons that sample various sub-regions of the bee's panoramic visual environment are spatially summed to generate a command signal that drives the streamlining response. Stimulation of the visual system with four monitors rather than two would then produce a stronger streamlining response. This hypothesis of summation is also consistent with our observation that presentation of forward image motion in the two front monitors and backward image motion in the two rear monitors – or *vice versa* – also evokes no flight (data not shown), presumably because the oppositely directed stimuli cancel each other out in each case.

If such spatial summation does indeed occur, the summation must not be linear because the response–speed curve that is obtained with four monitors cannot be predicted accurately simply by scaling the two-monitor curve by a factor of two. However, the four-monitor curve can be explained if we postulate that the streamlining response is driven by a saturating summation of the responses of the various movement-detecting neurons. The possibility is supported by the observation that the standard deviations of the responses obtained with the four-monitor stimulus are consistently smaller than those obtained with two monitors, at each of the tested speeds except for the lowest speed (172 deg s^{-1}) – a property that is characteristic of saturation at high response levels.

Can the observed saturation of the streamlining response at high contrasts be prevented by lowering the contrast of the visual stimulus to reduce the strength of the movement signal? Evidently not. The data in Fig. 5 show that, with the four-monitor stimulation, the response curves obtained for grating contrasts of 0.54, 0.36 and 0.29 are remarkably similar to and not significantly different from that obtained for a grating contrast of 0.72. This must mean that the responses of the movement-detecting neurons that drive the streamlining response are relatively insensitive to variations of stimulus contrast in the range of 0.29–0.72. This in turn implies that this invariance to contrast must come about through an invariance of each movement-detecting neuron's response to the stimulus for contrasts exceeding approximately 0.3. The lamina neurons, which are second-order neurons of the insect visual pathway, exhibit response saturation at contrasts exceeding 0.4 (Laughlin, 1981). If these lamina neurons provide the inputs to the movement-detecting neurons, their properties would partially account for the postulated contrast invariance. Indeed, individual movement-detecting neurons in the insect visual pathway show response invariance at contrasts exceeding approximately 0.3 (e.g. Dvorak et al., 1980). Thus, all of the properties of the streamlining response that have been observed so far can be explained by postulating phenomena occurring at two levels of the visual pathway: (1) contrast invariance of the responses of the movement-detecting neurons and (2) saturating summation of the responses of these movement-detecting neurons.

The finding that the streamlining response already attains a strength close to its maximum value for sinusoidal gratings with a Michelson contrast as low as 0.29 – which corresponds to a root mean square (r.m.s.) contrast of 0.20 – is very compatible with the fact that natural environments generally present r.m.s. contrasts in the range of 0.2–0.3 (e.g. Frazor and Geisler, 2006). Thus, the characteristics of the visually driven streamlining response are tailored to the properties of the natural environment.

Further evidence for the existence of nonlinear spatial summation in the process of movement detection comes from the experiments conducted using Virtual World 2. These experiments reveal, firstly, that the strength of the streamlining response does not depend upon the angular elevation of the stimulus (at least within the ±23 deg range of elevations that was investigated in these experiments). Thus, the response elicited by movement within an axial strip of the cylinder does not depend upon whether the strip is positioned in

the dorsal, ventral or equatorial field of view of the eyes. However, the response does depend upon the angular width of the strip: as the width of the strip is increased, the response increases at a less than linear rate, indicating a saturating spatial summation of the inputs that contribute to the response. Geometrical constraints imposed by the experimental design precluded investigation of the responses to stimuli at elevations outside the ±23 deg range. It is possible that stimulation from more dorsal or ventral sections of the tunnel may elicit responses of different strengths.

In contrast, examination of the strength of the response to changes in the azimuthal direction reveals a non-uniform sensitivity to the azimuthal position of the stimulus. The response is strongest in the lateral fields of view (AZ3) and weakest in the frontal and rear fields (AZ5). However, this variation in response displays a clear symmetry about the coronal plane (AZ2 and AZ4, AZ6 and AZ7). Part of the reason for the weak response in the frontal and rear regions of the visual field (AZ5) may be that the optic flow generated by the virtual tunnel decreases progressively in magnitude as the direction of view approaches the direction of (virtual) travel, which points towards the pole of the expanding flow field. Additionally, it is also possible that the frontal and rear regions of the visual field are inherently less sensitive to movement: our experiments cannot disentangle these two possibilities. The use of the virtual cylindrical tunnel as a stimulus permits an evaluation of the relative contributions of various sections of the tunnel to the streamlining response, but does not allow us to map the spatial variation of the response's sensitivity to movement *per se*. In principle, the latter can be probed by measuring the response elicited by various regions of the visual field by a small-field moving grating. However, such a procedure is likely to be impractical because our results so far suggest that small patches of movement do not elicit a measurable streamlining response.

If it is indeed true that the lateral (and dorsal and ventral) regions of the visual field are more sensitive to image motion than the frontal or rear regions, this would be advantageous because: (1) these are the regions of the visual field in which the optic flow induced by forward motion is likely to be the strongest, even when objects in the environment are far away; and (2) measurements of the optic flow in these regions are likely to provide the best estimates of forward flight speed because they are the least susceptible to spurious flow induced by rotations, such as yaw. The results presented in Figs 3–7 reveal that the streamlining response reaches its maximum value when the lateral image velocity approaches 300–400 deg s^{-1}. If we assume that, during flight in natural environments, the mean lateral distance of objects is, say, 1.5 m, we can calculate from Eqn 1 that such an image velocity would be experienced at flight speeds in the range of 7.8–10.5 m s^{-1}, which is typical of the cruising speeds that honeybees exhibit in outdoor flight [*ca.* 8 m s^{-1} (von Frisch, 1993), p. 189].

Our finding that the strength of the streamlining response does not vary with the angular elevation of the movement stimulus indicates that all sectors of the environment contribute to the bee's assessment of how rapidly it is flying through the environment, regardless of whether the sector is located dorsally, ventrally or laterally. This property may be functionally advantageous during flight through diverse environments, e.g. ranging from open fields to thick forests. The finding that stimulation within just one half of the total elevational extent of the cylindrical tunnel is sufficient to produce a nearly maximal response (Fig. 6) indicates that the streamlining response should be substantial even during flight in flat, open terrain, where only the ventral half of the bee's visual field would experience optic flow.

Functional significance of the streamlining response

The study by Nacthigall and Hanauer-Thiesser (Nacthigall and Hanauer-Thiesser, 1992), which measured the aerodynamic drag that is experienced by honeybees for various pitches of the abdomen, demonstrates clearly that drag is reduced when the abdomen is raised and is minimal when the abdomen is oriented horizontally, i.e. parallel to the direction of flight, when it presents a minimal cross-section to the horizontal airflow. Thus, the changes that we observed in abdominal pitch could indeed reflect a visually driven response that serves to reduce drag as the perceived speed through the environment is increased. Indeed, freely flying bees tend to hold the abdomen high when cruising and low when hovering or flying at slow speeds (Nachtigall et al., 1971). In real flight, however, bees should, at least in principle, be able to estimate their flight speed not just through visual cues but also through mechanosensory cues. For example, changes in abdominal pitch could be mediated by a reflex that is driven by sensing airspeed as signaled by the Johnston's organ at the base of the antennae and/or other wind-sensitive hairs on the head and body (Goodman, 2003). Additionally, the abdomen could simply be pushed up passively at higher flight speeds by the increased aerodynamic pressure acting on the underside of the abdomen and the legs (Nachtigall et al., 1971; Nachtigall and Hanauer-Thiesser, 1992). Notwithstanding these other possibilities, our experiments, conducted with tethered bees in still air, demonstrate clearly that vision plays an important role in tuning the posture of the body during flight.

Nachtigall and Hanauer-Thiesser have shown experimentally, by blowing wind at various velocities against the trunk of a honeybee, that the drag force is proportional to velocity$^{1.5}$ (Nachtigall and Hanauer-Thiesser, 1992). This implies that when a bee increases its flight speed from a value that is close to hover (say, 5 cm s^{-1}) to a value that is typical of cruise (say, 10 m s^{-1}), the drag would increase by a factor of approximately 2800 if the body did not change its posture or shape. The same study found that decreasing the angle of attack of the body from 20 to 0 deg can reduce the drag by approximately 50%, which would lead to a significant increase of flight speed and/or a significant saving of energy over a long flight. Thus, it would appear that actively raising the abdomen indeed produces a significant and beneficial streamlining effect.

Finally, the variation of posture with flight speed may represent more than just a streamlining response – it may reflect the fundamental means by which the insect adjusts its thrust and lift to achieve flight at various speeds. Horizontal flight at higher speeds requires the wings to produce not only increased thrust but also decreased lift, because the abdomen and the legs generate greater passive aerodynamic lift at higher speeds (Nachtigall and Hanauer-Thiesser, 1992). It has been suggested that, like the fruit fly *Drosophila* (Götz and Wandell, 1984; Zanker, 1988; Vogel, 1996), honeybees are unable to vary the direction of the net force vector that is generated by their wings relative to their body axis (Nachtigall et al., 1971; Esch et al., 1975; Taylor, 2001). If this is indeed the case, then the only way to increase flight speed – and to continue to fly horizontally – would be to decrease the angle of elevation of the force vector by pitching the thorax downwards and raising the abdomen (Nachtigall et al., 1971). Thus, our observed changes in abdominal pitch may reflect a part of this underlying strategy of flight control. However, exactly how changes in abdominal elevation can affect changes in the pitch of the thorax is not fully understood, although a model examining these changes has been proposed for *D. melanogaster* (Zanker, 1988), and the answer would depend partly on the (as yet undetermined) location of the insect's centre of gravity relative to the point of action of the net force vector

generated by the wings (Taylor, 2001). Götz et al. suggest that turning responses (yaw) during flight may be facilitated by ruddering actions of the abdomen (deflections of the abdomen in the horizontal plane) in addition to differential changes in wing stroke amplitude and alterations in leg posture (Götz et al., 1979).

One needs to be mindful of the possibility that a tethered insect can display motor behaviors that are different from those observed in free flight (Dudley, 2000; Fry et al., 2005). Fry et al. observed that tethered *D. melanogaster* exhibit thrust and lift magnitudes and patterns of wing motion that are different from those exhibited by freely flying individuals (Fry et al., 2005). Thus, it is possible that the act of tethering a flying insect causes it to produce unnatural responses that are directed at overcoming the effects of the restraints imposed by the tether. What we do find, however, is that in tethered bees, the abdominal pitch decreases with increased (apparent) flight speed, just as it does in freely flying bees (Nachtigall et al., 1971).

It should be noted that the responses described in the present study have been obtained using an 'open loop' mode of experimentation in which the insect is responding to the stimulus that it receives, but is unable to influence the stimulus. Our experiments reveal that body posture is strongly influenced by the visual stimulus, but they do not tell us whether an unrestrained bee in free flight controls its flight speed (and, therefore, the image speed that it experiences) by adjusting its body posture. Further studies, conducted using a 'closed loop' paradigm in which the tethered insect is able to freely adjust the pitch of its body, and where the measured thrust and lift are used to appropriately control the motion of the visual panorama as well as the airflow, should provide a more complete understanding of the phenomenon that we have uncovered here.

ACKNOWLEDGEMENTS

We appreciate the valuable suggestions from the anonymous referees for extending the study to include a detailed investigation of the sensitivity of the streamlining response to movement in different regions of the visual field. This work was supported partly by grants from the ARC Special Research Initiative on Thinking Systems (TS0669699), the ARC Centre of Excellence in Vision Science (CE0561903), the US Asian Office of Aerospace R&D (award no. AOARD064092) and by a Queensland Smart State Premier's Fellowship.

REFERENCES

Bailey, J. (1997). *How Fish Swim*. New York: Benchmark Books.
Baird, E., Srinivasan, M. V., Zhang, S. and Cowling, A. (2005). Visual control of flight speed in honeybees. *J. Exp. Biol.* **208**, 3895-3905.
Batchelor, G. K. (2000). *An Introduction to Fluid Dynamics* (Cambridge Mathematical Library, 2nd edn). Cambridge: Cambridge University Press.
Chadwick, L. E. (1953). The flight muscles and their control. In *Insect Physiology* (ed. K. D. Roeder), pp. 648-655. New York: Wiley.
Chittka, L., Vorobyev, M., Shmida, A. and Menzel, R. (1993). Bee colour vision – the optimal system for the discrimination of flower colours with three spectral photoreceptor types? *In Sensory Systems of Arthropods* (ed. K. Weise, F. G. Gribakin, A. G. Popov and G. Renninger), pp. 211-218. Basel: Birkhauser Verlag.
Collett, T., Nalbach, H.-O. and Wagner, H. (1993). Visual stabilization in arthropods. In *Visual Motion and its Role in the Stabilization of Gaze* (ed. F. Miles and J. Wallman), pp. 239-263. Amsterdam: Elsevier.
David, C. T. (1978). The relationship between body angle and flight speed in free-flying *Drosophila*. *Physiol. Entomol.* **3**, 191-195.
David, C. T. (1979). Optomotor control of speed and height by free-flying *Drosophila*. *J. Exp. Biol.* **82**, 389-392.
David, C. T. (1982). Compensation for height in the control of groundspeed by *Drosophila* in a new 'barber's pole' wind tunnel. *J. Comp. Physiol. A* **147**, 485-493.
Dudley, R. (2000). *The Aerodynamics of Insect Flight*. Princeton: Princeton University Press.
Dudley, R. and Ellington, C. P. (1990). Mechanics of forward flight in bumblebees. I. Kinematics and morphology. *J. Exp. Biol.* **148**, 19-52.
Dvorak, D., Srinivasan, M. V. and French, A. S. (1980). The contrast sensitivity of fly movement-detecting neurons. *Vision Res.* **20**, 397-407.
Egelhaaf, M., Grewe, J., Karmeier, K., Kern, R., Kurtz, R. and Warzecha, A. (2004). Novel approaches to visual information processing in insects: case studies on neuronal computations in the blowfly. In *Methods in Insect Sensory Neuroscience* (ed. T. A. Christensen), pp. 185-212. Boca Raton, London and New York: CRC Press.
Esch, H., Nachtigall, W. and Kogge, S. N. (1975). Correlations between aerodynamic output, electrical activity in the indirect flight muscles and wing positions of bees flying in a servomechanically controlled wind tunnel. *J. Comp. Physiol.* **100**, 147-159.
Fraenkel, G. (1932). Untersuchungen über die Koordination von Reflexen und automatisch-nervösen Rhythmen bei Insekten. I. Die Flugreflexe der Insekten und ihre Koordination. *Zeitschr. Vgl. Physiol.* **16**, 371-393.
Frazor, R. A. and Geisler, W. S. (2006). Local luminance and contrast in natural images. *Vision Res.* **46**, 1585-1598.
Fry, S. N., Sayaman, R. and Dickinson, M. H. (2005). The aerodynamics of hovering flight in *Drosophila*. *J. Exp. Biol.* **208**, 2303-2318.
Fry, S. N., Rohrseitz, N., Straw, A. D. and Dickinson, M. H. (2009). Visual flight speed control in *Drosophila melanogaster*. *J. Exp. Biol.* **212**, 1120-1130.
Goodman, L. (2003). *Form and Function in the Honeybee*. Cardiff: International Bee Research Association.
Götz, K. G. (1965). Die optischen Übertragungseigenschaften der Komplexaugen von *Drosophila*. *Kybernetik.* **2**, 215-221.
Götz, K. G. and Wandel, U. (1984). Optomotor control of the force of flight in *Drosophila* and *Musca*.II. Covariance of lift and thrust in still air. *Biol. Cybern.* **51**, 135-139.
Götz, K. G., Hengstenberg, B. and Biesinger, R. (1979). Optomotor control of wing beat and body posture in *Drosophila*. *Biol. Cybern.* **35**, 101-112.
Krapp, H. G. and Hengstenberg, R. (1996). Estimation of self-motion by optic flow processing in single visual interneurons. *Nature* **384**, 463-466.
Laughlin, S. B. (1981). A simple coding procedure enhances a neuron's information capacity. *Z. Naturforsch.* **36C**, 910-912.
Menzel, R. and Blakers, M. (1976). Color receptors in the bee eye-morphology and spectral sensitivity. *J. Comp. Physiol.* **108**, 11-13.
Michelson, A. A. (1927). *Studies in Optics*. Chicago: The University of Chicago Press.
Nachtigall, W. and Hanauer-Thieser, U. (1992). Flight of the honeybee. V. Drag and lift coefficients of the bee's body; implications for flight dynamics. *J. Comp. Physiol. B* **162**, 267-277.
Nachtigall, W., Widmann, R. and Renner, M. (1971). Uber den "ortsfesten" freien Flug von Bienen in einem Saugkanal. *Apidologie* **2**, 271-282.
Reichardt, W. (1969). *Processing of Optical Data by Organisms and by Machines*. New York: Academic Press.
Schmidt-Nielsen, K. (1984). *Scaling: Why is Animal Size so Important?* Cambridge and New York: Cambridge University Press.
Srinivasan, M. V. and Bernard, G. D. (1977). The pursuit response of the housefly and its interaction with the optomotor response. *J. Comp. Physiol. A* **115**, 101-117.
Srinivasan, M. V. and Zhang, S. W. (1997). Visual control of honeybee flight. In *Orientation and Communication in Arthropods* (ed. M. Lehrer), pp. 95-114. Basel, Boston and Berlin: Birkhauser Verlag.
Srinivasan, M. V., Lehrer, M., Kirchner, W. and Zhang, S. W. (1991). Range perception through apparent image speed in freely flying honeybees. *Vis. Neurosci.* **6**, 519-535.
Srinivasan, M. V., Zhang, S. W. and Chandrashekara, K. (1993). Evidence for two distinct movement-detecting mechanisms in insect vision. *Naturwissenschaften* **80**, 38-41.
Srinivasan, M. V., Zhang, S. W., Lehrer, M. and Collett, T. (1996). Honeybee navigation *en route* to the goal: visual flight control and odometry. *J. Exp. Biol.* **199**, 237-244.
Srinivasan, M. V., Zhang, S. W., Chahl, J. S., Barth, E. and Venkatesh, S. (2000). How honeybees make grazing landings on flat surfaces. *Biol. Cybern.* **83**, 171-183.
Tammero, L. F. and Dickinson, M. H. (2002). Collision-avoidance and landing responses are mediated by separate pathways in the fruit fly, *Drosophila melanogaster*. *J. Exp. Biol.* **205**, 2785-2798.
Taylor, G. K. (2001). Mechanics and aerodynamics of insect flight control. *Biol. Rev.* **76**, 449-471.
Willmott, A. P. and Ellington, C. P. (1997). The mechanics of flight in the hawkmoth *Manduca sexta*. I. Kinematics of hovering and forward flight. *J. Exp. Biol.* **200**, 19-52.
Vogel, S. (1966). Flight in *Drosophila*. I. Flight performance of tethered flies. *J. Exp. Biol.* **44**, 567-578.
von Frisch, K. (1993). *The Dance Language and Orientation of Bees*. Cambridge, MA: Harvard University Press.
Zanker, J. M. (1988). On the mechanism of speed and altitude control in *Drosophila melanogaster*. *Physiol. Entomol.* **13**, 351-361.